Modes in Unstable Optical Resonators and Lens Waveguides

ANTHONY E. SIEGMAN, FELLOW, IEEE, AND RAYMOND ARRATHOON

Abstract—Optical resonators and/or lens waveguides are "unstable" when they have divergent focusing properties such that they fall in the unstable region of the Fox and Li mode chart. Although such resonators have large diffraction losses, their large mode volume and good transverse-mode discrimination may nonetheless make them useful for high-gain diffraction-coupled laser oscillators. A purely geometrical mode analysis (valid for Fresnel number $N = \infty$) shows that the geometrical eigenmodes of an unstable system are spherical waves diverging from unique virtual centers. As Burch has noted, the higher-order transverse modes in the geometrical limit have the form $u_n(x) = x^n$ with eigenvalues $\gamma_n = 1/M^{n+1/2}$, where M is the linear magnification of the spherical wave per period. The higher-order modes have nodes on-axis only, and there is substantial transverse-mode discrimination. More exact computer results for finite N show that the spherical-wave phase approximation remains very good even at very low N, but the exact mode amplitudes become more complicated than the geometrical results. The exact mode loss versus N exhibits an interesting quasi-periodicity, with $n = 0$ and $n = 2$ mode degeneracy occurring at the loss peaks. Defining a new equivalent Fresnel number based on the actual spherical waves rather than plane waves shows that the loss peaks occur at integer values of N_{eq} for all values of M.

Introduction

ALMOST all the studies of optical resonators carried out thus far are concerned either with *stable* resonators, which lie in the stable region of the Fox and Li mode chart and have Gaussian normal modes, or with special limiting cases on the boundary of the stability region, such as the planar resonator.[1] The present paper, by contrast, is concerned with *unstable* optical resonators—i.e., resonators which fall well into the unstable region of the Fox and Li mode chart. Such resonators do have large diffraction losses. However, with reasonable design parameters these losses do not exceed the gains per pass available in many useful laser systems, so that laser operation using unstable resonators is entirely possible. There are, in fact, at least three reasons why unstable optical resonators may be attractive for such laser applications:

1) Unstable resonators can have *large mode volumes* even in very short resonators.
2) The unstable configuration is readily adapted to adjustable *diffraction output coupling.*
3) The analysis indicates that unstable resonators should have very substantial *discrimination against higher-order transverse modes.*

Manuscript received November 30, 1966; revised January 16, 1966. This work was supported by the U. S. Air Force Avionics Laboratory through Contract AF 33(615)-1411 with Stanford University.

The authors are with the Department of Electrical Engineering, Stanford University, Stanford, Calif.

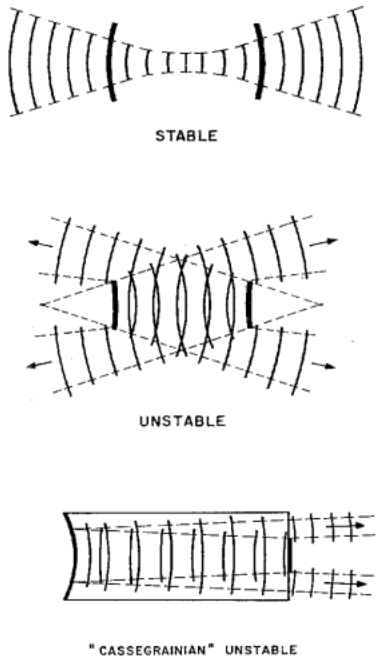

Fig. 1. Examples of elementary "stable" and "unstable" optical resonators.

Figure 1 illustrates a typical stable resonator, a general symmetric unstable reasonator, and a specific "Cassegrainian" unstable resonator with the output diffraction coupled entirely from one end.

The elementary properties of unstable optical resonators were described in an earlier paper.[2] In the present paper, this elementary geometrical description is extended to give the higher-order modes of unstable optical resonators and lens waveguides. In addition, the results are presented of some exact numerical calcuations which indicate the range of validity of the geometrical analysis and the nature of the approximations in the geometrical analysis. A new equivalent Fresnel number for unstable resonators is defined, and the relationship of mode losses and mode configurations to this parameter is demonstrated.

Geometrical Analysis

Figure 2 shows the geometry and the basic mode configuration of an unstable lens waveguide. For simplicity, the resonator problem will be analyzed in terms of the equivalent lens waveguide shown in Fig. 2. The analysis will also be limited to the symmetric case, i.e., every lens in the unstable lens waveguide is assumed identical, rather than every second lens as in the general unsymmetric case. In developing the analysis reference planes

z_a and z_b located just *before* each lens in the lens waveguide will be used.[1]

Let $u^a(y)$ and $u^b(x)$ denote the complex scalar field amplitude as a function of the transverse coordinates of these reference planes. Then a wave in passing through a lens at a point displaced by a distance y from the axis will suffer a phase shift $\Delta\phi_{\text{lens}}(y) = ky^2/2f = (g-1)ky^2/L$, where $g \equiv (1 + L/2f)$ is the g parameter widely used in optical resonator analyses. In addition, in traveling from a point y on one plane to a point x at the next reference plane an axial distance L farther along, the wave will suffer an additional geometrical phase shift given (to the Fresnel degree of approximation) by $\Delta\phi_{\text{path}}(x, y) = (k/2L)(x - y)^2$. If we then consider for simplicity the *strip* resonator case (i.e., cylindrical waves and lenses), Huygens' principle relates the field $u^b(x)$ at plane $z = z_b$ to the field $u^a(y)$ at plane $z = z_a$ by

$$u^b(x) = \sqrt{\frac{j}{L\lambda}} \int_{-a}^{a} e^{-j(\pi/L\lambda)[x^2+(2g-1)y^2-2xy]} u^a(y)\, dy \qquad (1)$$

where $2a$ is the width of the lens aperture. This becomes an integral equation for the normal modes of the resonator or lens waveguide if we require that the amplitude at the second plane be

$$u^b(x) = \gamma u^a(x) \qquad (2)$$

and drop the a superscripts as superfluous. Solutions to this integral equation give the eigenmodes $u_n(x)$ and eigenvalues γ_n of the unstable lens waveguide.

From the previous elementary analysis of the unstable optical resonator,[2] we expect the normal modes of this lens waveguide to consist of spherical (or cylindrical) waves diverging from virtual centers located a unique distance behind each lens. It is convenient to extract out this expected basic spherical wave from both sides of this equation by writing the wave functions $u(x)$ in the form

$$u(x) = v(x)e^{-j(\pi/L\lambda)[(M-1)/M]x^2}. \qquad (3)$$

The parameter M which appears in this expression is the linear magnification of the spherical wave in passing from one lens to the next. By manipulating the expressions in the earlier paper,[2] this linear magnification can be expressed in the form

$$M = \frac{\sqrt{g+1} + \sqrt{g-1}}{\sqrt{g+1} - \sqrt{g-1}}. \qquad (4)$$

The radius of curvature of the geometrical eigenwave at the reference plane just before the lens is then $[M/(M-1)]L$.

[1] The analytical development of the integral equation can be carried out most succinctly using reference planes located either *just before* or *just after* each lens. However, the same final integral equation, (5), is obtained whether one uses these reference planes or reference planes located *in the middle of* the lenses as indicated in Fig. 2, provided that the spherical wave which is extracted from $u(x)$ has the appropriate curvature for the particular planes chosen.

With the spherical-wave phase variation extracted, the integral equation takes the form

$$\gamma v(x) = \frac{\sqrt{jN}}{a} \int_{-a}^{a} e^{-i\pi MN(y-x/M)^2/a^2} v(y)\, dy \qquad (5)$$

where $N \equiv a^2/L\lambda$ is the Fresnel number widely used in optical resonator analyses. This equation is the basic integral equation to be solved for the modes of the unstable resonator or lens waveguide.[1]

It is apparent from the exponent in this equation that, as illustrated in Fig. 2, the principle contribution to the wave amplitude at a point x at the second reference plane comes from the region centered around a point $y = x/M$ on the first reference plane. As a first approximation, therefore, we expand the function $v(y)$ inside the integral sign in the Taylor series

$$v(y) = v(x/M) + v'(x/M) \times (y - x/M) + \cdots \qquad (6)$$

and keep only the first term in this series. The integral in (5) then takes the form of a Fresnel integral. Evaluation of this Fresnel integral in the limit $N \to \infty$ leads to the simple *purely geometrical* form on the "integral equation:"

$$\gamma v(x) = \frac{1}{\sqrt{M}} v\left(\frac{x}{M}\right). \qquad (7)$$

This result is, in fact, obvious from geometrical optics. The factor of $1/\sqrt{M}$ arises from the fact that, in the strip case, the energy leaving the first plane is expanded over an area increased by a factor of M at the second plane. It is also readily apparent by inspection that the eigenfunctions and eigenvalues of (7) are given by the simple forms

$$v_n(x) = x^n, \qquad \gamma_n = \frac{1}{M^{n+1/2}}. \qquad (8)$$

The amplitudes of the lowest- and high-order *geometrical* modes of an unstable optical resonator or lens waveguide in the strip case thus have the simple forms shown in Fig. 3. Each function x^n, when linearly expanded and then trimmed to the same aperture width, obviously still has the same form x^n. It is also apparent from these sketches that the higher-order transverse modes will have substantially higher losses per pass, because the energy in these modes is concentrated near the edges of the resonator and is thus more rapidly lost in a single bounce. Thus, excellent transverse mode discrimination is predicted for laser applications of these modes.

It is also interesting to note the substantial differences between these modes and the well-known modes of stable optical resonators. In particular, the unstable resonator modes have no nulls located anywhere except on the axis of the resonator. Any node located off the axis of the resonator would obviously "walk out" of the resonator in a single pass or at most a few passes.

It seems apparent without derivation that the equivalent geometrical "integral equation" for a spherically symmetric lens waveguide will be of the form

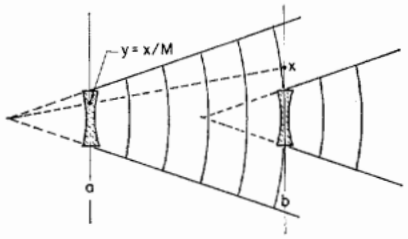

Fig. 2. Geometry for the unstable lens waveguide analysis.

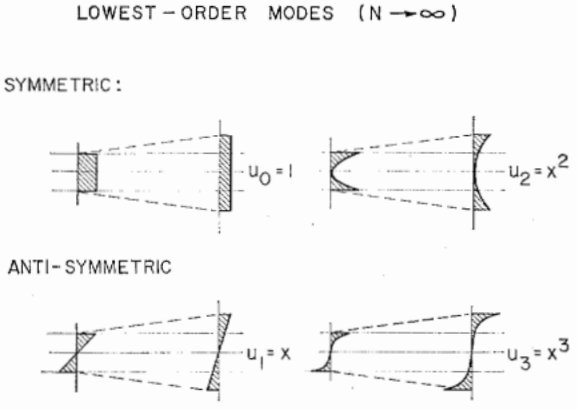

Fig. 3. The first four geometrical eigenmodes of an unstable resonator.

$$\gamma v(r, \theta) \approx \frac{1}{M} v(r/M, \theta). \tag{9}$$

The geometrical eigensolutions and eigenvalues for this case will be

$$v_n(r, \theta) = r^n \Theta(\theta), \qquad \gamma_n = \frac{1}{M^{n+1}} \tag{10}$$

where $\Theta(\theta)$ can be any arbitrary function of θ, and where there will clearly be some degeneracy in the eigensolutions related to the θ indeterminacy which will not be explored further here. These solutions can have radial nodal lines, but otherwise will have no nodes off axis. The discrimination against the higher-order transverse modes relative to the lowest-order or uniform mode is even higher in this spherical or *disk* case than in the strip case. Figure 4 is a plot of the loss per bounce versus resonator parameters for the lowest-order and several higher-order modes, for the case of a disk resonator with the geometry shown in the inset, as predicted by the elementary geometrical analysis. The very high degree of transverse mode discrimination expected in unstable optical resonators is apparent. This result has yet to be verified experimentally, and is partially negated by more exact numerical calculations to be presented in the following section. Nonetheless, it represents one of the principle reasons for continued interest in unstable optical resonators.

As was noted in the earlier paper,[2] these results show that in the geometrical limit neither the mode patterns nor the mode losses depend directly upon the mirror sizes. It is possible, therefore, to have a relatively large diameter mode even in a relatively short resonator. Large-mode volume in a short resonator, which is difficult with

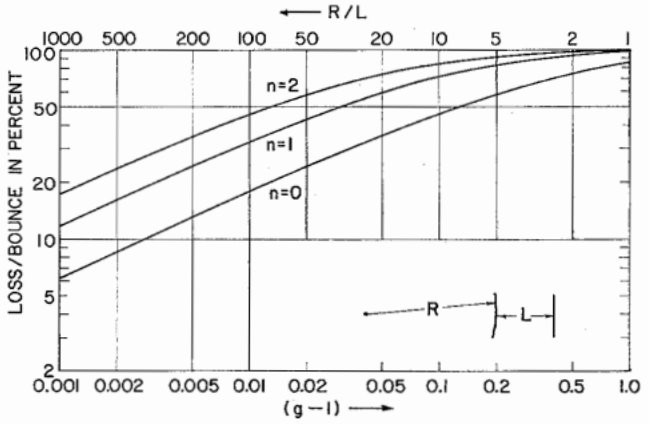

Fig. 4. Loss per bounce according to the purely geometrical analysis for the three lowest-order modes of the unstable resonator configuration shown.

stable resonator configurations can thereby be obtained. This forms another major advantage of the unstable resonator approach.

Exact Numerical Calculations

In order to obtain further information about the modes and mode losses of unstable optical resonators, the exact integral equation for the strip case given in (1) has been solved numerically by digital computation in the fashion first developed by Fox and Li.[3] The results of these exact numerical computations can be compared and contrasted with the results of the elementary geometrical analysis.

As a first result Fig. 5 shows typical plots of the *phase* of the lowest-order eigenfunction versus radius, as derived both from the exact iterative numerical calculation procedure and from the geometrical analysis for three relatively low values of the Fresnel number N. The significant result here is that the exact numerical results are very well approximated by the quadratic phase variation of the cylindrical wave which is derived from the geometrical analysis, even at relatively low values of the Fresnel number. It is concluded that the spherical-wave approximation is a surprisingly good approximation at least for the *phase* variation of the waves in an unstable resonator or waveguide.

Figure 6 presents results for the *amplitude* variation of the lowest-order and next highest-order symmetric modes in an unstable resonator as derived from the exact computer calculations. It is evident from these results that the geometrical analysis is less successful in predicting the transverse *amplitude* variation of the modes, particularly at lowest Fresnel numbers. The exact mode patterns contain a large number of ripples, which are presumably related to the Fresnel zones at one reference plane as seen from the succeeding reference plane.[3]

Figure 7 (which is repeated from the first unstable resonator paper) is a plot of the loss per bounce of the lowest-order mode in an unstable strip resonator as obtained from exact numerical solutions, compared with the geometrical loss results, which are indicated by the dashed

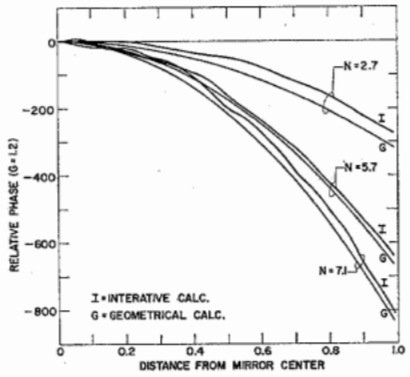

Fig. 5. Phase variation relative to the mirror surface of the lowest-order mode versus radius as obtained from the geometrical analysis (G) and from an exact iterative computer solution (I) for three typical values of Fresnel number N.

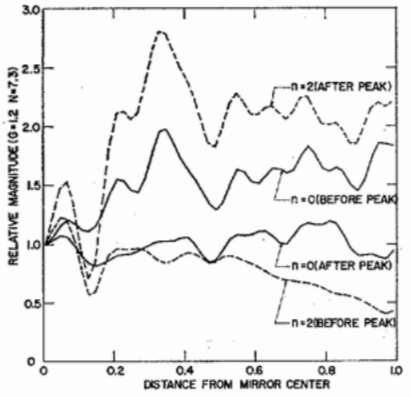

Fig. 6. Amplitude variations of the lowest-order and next higher-order symmetric modes versus radius, as obtained from the exact computer calculation, for $g = 1.2$ and for two closely adjacent values of N, just below and just above a "loss peak." These may be compared with the geometrical predictions in Fig. 3.

lines. It is apparent that there is an interesting quasi-periodic ripple in the exact loss versus Fresnel number curves. Some insight into the nature of this ripple in the loss versus Fresnel number curve has been obtained from the following results.

The Fresnel number N, which is widely used as a parameter in resonator analyses, represents physically the number of Fresnel zones of a plane wave filling one mirror as seen from the center of the following mirror or lens. In the unstable case, however, it is apparent that the wave leaving one mirror and traveling to the next mirror is not a plane wave but a spherical (or cylindrical) wave. It would seem more natural, therefore, to define a Fresnel number based in some way on the number of Fresnel zones on the actual spherical wave at one mirror as seen from the center of the following mirror. By a somewhat devious route such as equivalent Fresnel number may be defined as

$$N_{eq} = \frac{1}{2}\left(M - \frac{1}{M}\right)N. \tag{11}$$

When the exact loss per bounce versus Fresnel number curves of Fig. 7 are replotted against this equivalent Fresnel number rather than the usual Fresnel number, these loss curves take on the very regular form shown in

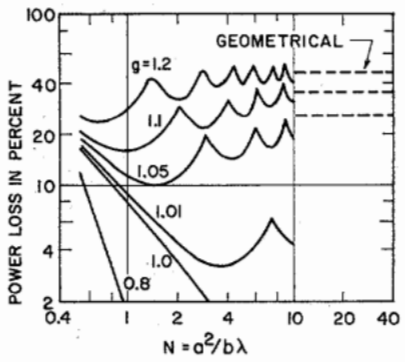

Fig. 7. Comparison of loss per bounce versus Fresnel number N for the strip case as obtained from the exact numerical computations (solid lines) and the geometrical analysis (dashed lines). (Data from this work and from [4].)

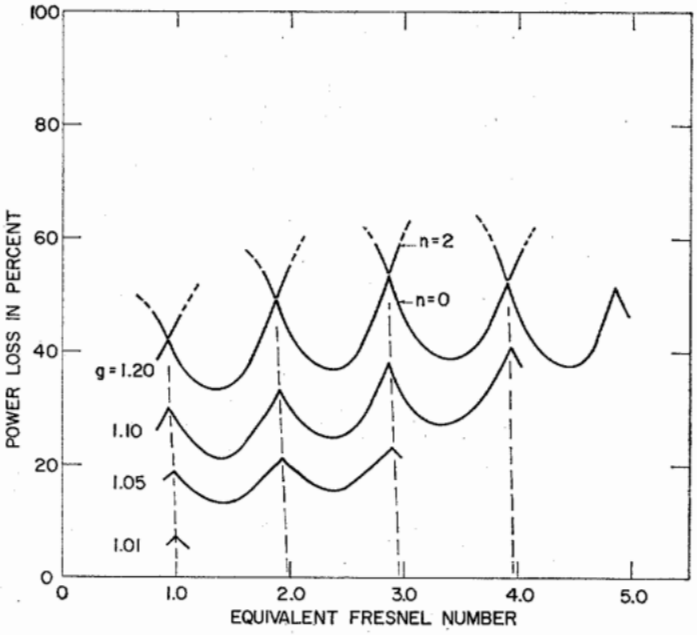

Fig. 8. Exact unstable loss-per-bounce curves from Fig. 7, replotted against the new equivalent Fresnel number. Some exact results for the loss of the next higher-order symmetric ($n = 2$) mode are also shown (dashed curves).

Fig. 8. (The curves shown in Fig. 8 have been taken in part from Fox and Li's published curves[4] and in part from our own computer results which have extended and in general verified their results.) It is apparent that the loss peaks in these curves occur at very nearly integral values of the equivalent Fresnel number N_{eq} almost entirely independently of the value of g. (The slight departure from the exact integral values of the peaks may possibly be due to the fact that, as shown in Fig. 5, the exact computer results appear to have a slight but systematic difference in curvature from the geometrically predicted spherical waves.)

The physical significance of the equivalent Fresnel number N_{eq} as defined in (11) remains somewhat obscure. The Fresnel number N as conventionally defined, is equal to the additional path length per pass in half wavelengths for a ray which travels from mirror center to mirror edge (path length $= L + N\lambda/2$), as compared with a ray which travels from mirror center to mirror center (path

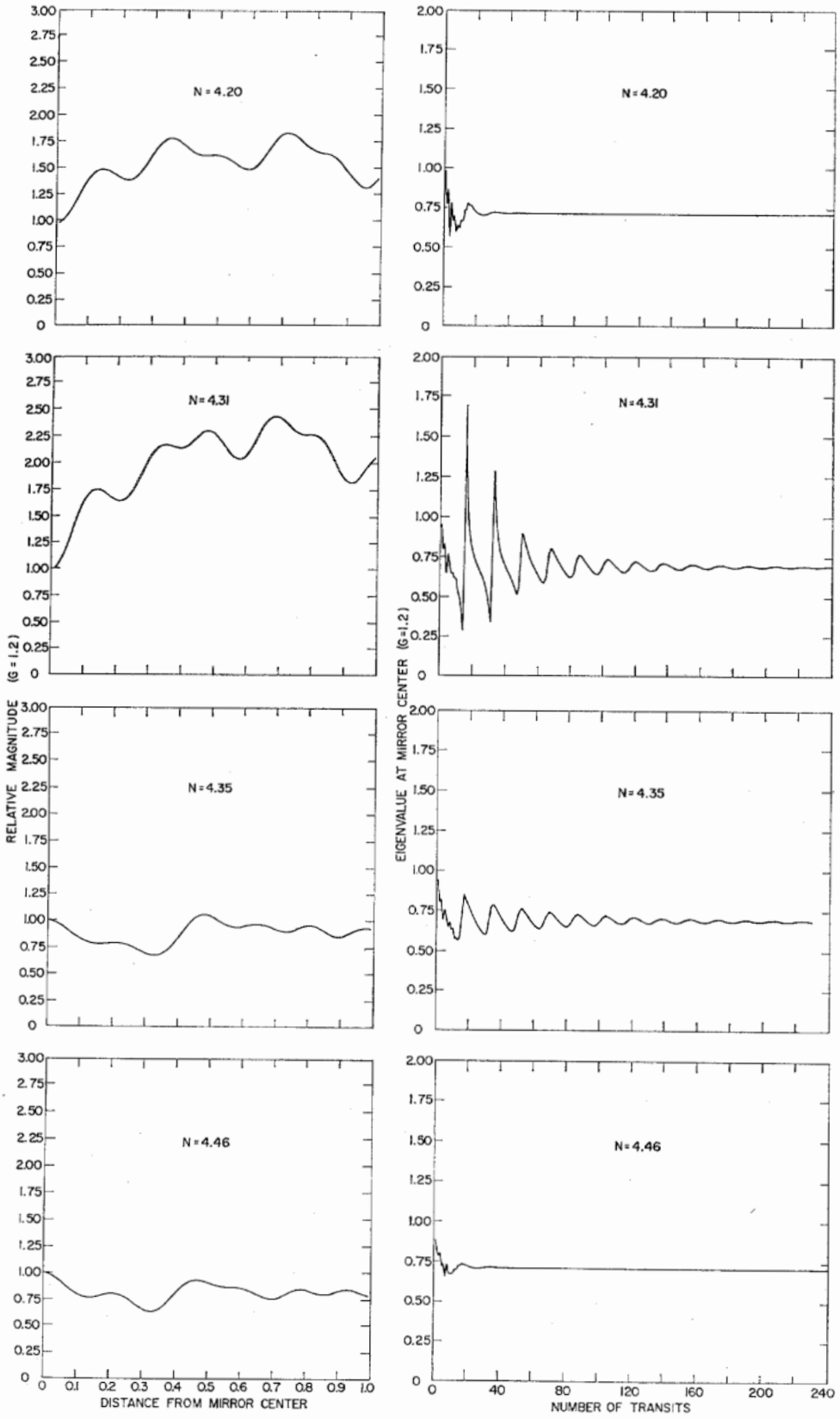

Fig. 9. Typical computer results for four closely spaced values of N, two on either side of the "loss peak" located at $g = 1.2$, $N = 4.5$. The left-hand column shows the final steady-state amplitude pattern of the lowest-order ($n = 0$) mode. The right-hand column shows the attenuation per bounce as a function of bounce number during the course of each calculation, starting with an initially uniform distribution.

length = L). Our equivalent Fresnel number N_{eq} is equal, among other things, to the additional path length in half-wavelengths that a ray would travel in going from the *virtual center* behind one mirror to the opposite mirror's edge as compared to a ray going from the same virtual center to the opposite mirror's center. In terms of Fresnel zones and the lens waveguide model, N_{eq} has the rather mystifying interpretation of being equal to the number of Fresnel zones of the geometrically predicted wave at the midplane of one lens, as seen from the center of the next lens, *not* taking into account the phase shift that will be added to that wave as it travels from the midplane of the lens on through the front half of the lens. Note that N_{eq} does *not* approach N as the resonator parameters approach the stable region boundary ($M \rightarrow 1$).

Further interesting results are obtained when the computer calculations are carried out for points located closely adjacent to, and on both sides of, any of the loss peaks shown in Figs. 7 or 8. As an example, Fig. 9 shows typical computer results for four closely spaced Fresnel numbers, two located just to the left and two located just to the right of the loss peak at $g = 1.2$, $N = 4.5$. The left-hand column shows the amplitude variation of the steady-state $n = 0$ mode pattern from the center to the edge of the mirror (with the center amplitude arbitrarily set at unity), while the right-hand column shows the variation of the attenuation per bounce at the center of the mirror as a function of the number of bounces during the course of the iterative computer calculation. From the left-hand column, it is apparent that there is a very distinct and sudden change in the character of the lowest-order transverse mode pattern upon passing through the loss peak. No such distinctive change in character is apparent in the phase variation across the mirror for the same cases.

The right-hand column represents the evolution to a final steady-state which takes place in the usual computer procedure, when an initial amplitude distribution (uniform, for lack of anything better) is started out in the lens waveguide. The iterative computer procedure causes this initially uniform distribution to evolve eventually into the steady-state lowest-order mode distribution shown in the left-hand column. The right-hand column plots essentially the attenuation at the center of the mirror during each successive bounce, as a function of the number of bounces during this convergence procedure. As Fox and Li earlier noted,[3] the ringing or beating which is evident in some of these curves represents physically a periodic constructive and destructive interference between the dominant lowest-order ($n = 0$) mode in the resonator and a certain component of the next higher-order ($n = 2$) transverse mode, which is excited by the initial uniform distribution and which slowly dies out during the computational process because of its higher loss per bounce. By a combined analytical and computational procedure, it is possible to extract from curves such as these both the mode pattern and the loss per bounce of the next higher-order ($n = 2$) mode as well as the lowest-order or dominant mode. It is apparent from Fig. 9 that the higher-order mode beats with the lowest-order mode for a longer period for Fresnel numbers very close to the loss peak, indicating that the losses of the two modes are very nearly equal. Losses of the higher-order or $n = 2$ mode derived in this fashion have also been included in Fig. 8. It is evident that the loss *peak* in the $n = 0$ mode coincides with a loss *minimum* for the $n = 2$ mode and that the two loss curves essentially intersect at this point. Operation at or near these points in a practical laser would obviously be very undesirable, since the mode discrimination between $n = 0$ and $n = 2$ modes would then become vanishingly small.

Finally, Fig. 10 plots the loss of the *lowest symmetrical* ($n = 0$) and the *lowest antisymmetrical* ($n = 1$) modes versus equivalent Fresnel number N_{eq} for a typical case ($g = 1.2$, strip mirrors). It appears that the periodic loss variations characteristic of the symmetric modes are absent, or at least greatly suppressed, for the antisymmetric mode. There is, however, uniformly good loss discrimination between the $n = 0$ and $n = 1$ modes. The geometrically predicted losses are also indicated on the plot, showing that the antisymmetric mode has considerably less loss than predicted by the geometrical analysis. Examination of the exact computed mode patterns shows that the $n = 0$ mode pattern is basically uniform in amplitude across the mirror, with some ripple, so that the geometrical analysis provides a fairly good approximation to the exact mode loss. The exact mode

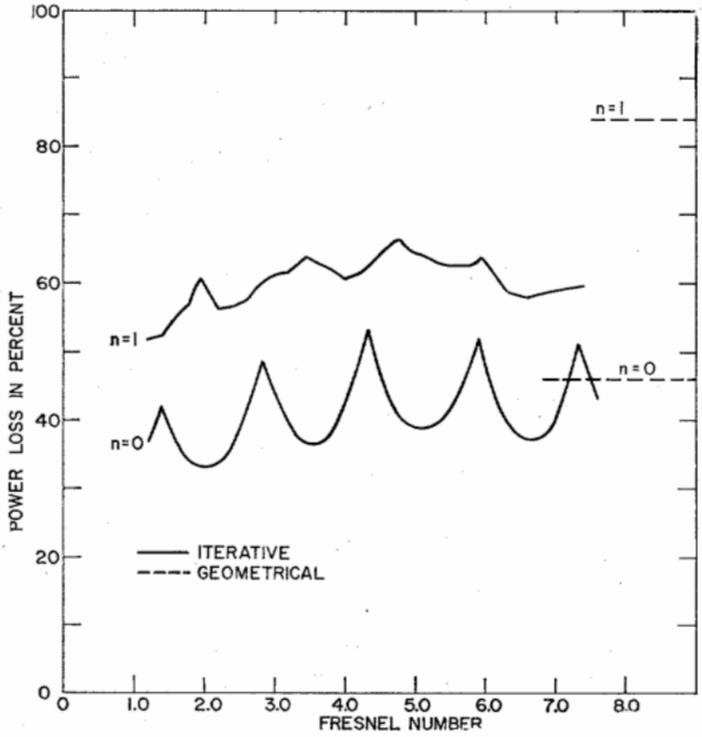

Fig. 10. Loss per bounce in percent versus Fresnel number N for the lowest-order symmetric ($n = 0$) and antisymmetric ($n = 1$) modes for a typical strip resonator case. The solid lines are exact, while the dashed lines represent the geometrical approximation.

pattern for the $n = 1$ mode, however, is not well approximated by the linear geometrical approximation of Fig. 3. The mode amplitude is, of course, zero at the mirror center, and varies more or less linearly with transverse position over approximately the middle third of the mirror; but the $n = 1$ mode amplitude is then basically constant rather than linear, with sizable ripples over the remainder of the cross section. As a consequence, the exact losses are substantially less than the geometrically predicted value. The $n = 1$ mode pattern makes good use of its ability to readjust its amplitude and phase distribution through diffraction in such a way as to minimize its diffraction losses.

Far-Field Pattern Experiment

Experiments intended to test the mode patterns and mode characteristics of unstable optical resonators in more detail are now being undertaken, but no results have been obtained as yet. However, the following related experiment has been performed. The output from an unstable resonator laser is most conveniently obtained as a diffraction-coupled ring of light emerging around the mirror at one end of the laser cavity. The similarity of this configuration to a Cassegrainian antenna structure suggested that this be called a Cassegrainian laser configuration. As in the Cassegrainian antenna case, the main lobe of the far-field pattern of this near-field output distribution has a strong main lobe on axis. However, in order to examine the far-field diffraction pattern of this aperture in more detail the far-field diffraction of such an annular ring was simulated using the annular mask shown in Fig. 11. The mask was prepared by careful photoetching of a silver film evaporated onto a glass plate. The annulus thus prepared was illuminated by the uniform central portion of an expanded and collimated single-mode gas laser beam. Figure 12 shows two examples of the resulting far-field diffraction pattern of this annulus. The main central lobe in the center of the pattern is greatly overexposed in order to bring out the interesting outer ring pattern. The inner and outer diameters of the annulus in Fig. 11 have a very nearly 2-to-1 ratio. From Babinet's principle, the far-field intensity pattern of this annulus consists of a superposition of the Airy amplitude function of the outer diameter, minus the Airy amplitude function of the inner diameter, with this difference then squared.[5] The diffraction rings of these two Airy patterns have radial periods differing by the diameter ratio of 2-to-1, and a closer examination shows that this results in a constructive and destructive interference between the patterns which repeats every fourth ring. As a result the rings in Fig. 12 show a repetitive pattern of two enhanced rings followed by two missing rings persisting over several cycles. The additional structure appearing in the photograph represents multiple reflections and the other imperfections in the optical components used.

One parameter of interest for a laser oscillator is the on-axis brightness of the laser mode in the far field. In assessing the performance of an unstable resonator by this criterion, it would seem fair to compare a diffraction-coupled unstable resonator against a conventional resonator configuration with semitransparent mirror coupling, assuming the same total output power and the same outer diameter for the laser mode in each case. In the absence of a more definite criterion, a uniformly illuminated annular aperture of outer diameter a and inner diameter ϵa will be compared with a uniformly illuminated disk of outer diameter a with the same total transmitted power in both cases. The on-axis brightness ratio is then

$$\frac{I_0(\epsilon)}{I_0(0)} = (1 - \epsilon^2) = 2\delta - \delta^2$$

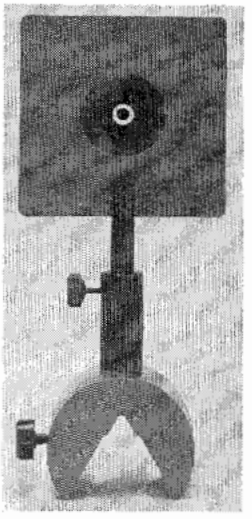

Fig. 11. An annular aperture with nearly 2-to-1 outer-inner diameter ratio to simulate the output of a diffraction-coupled unstable-resonator laser.

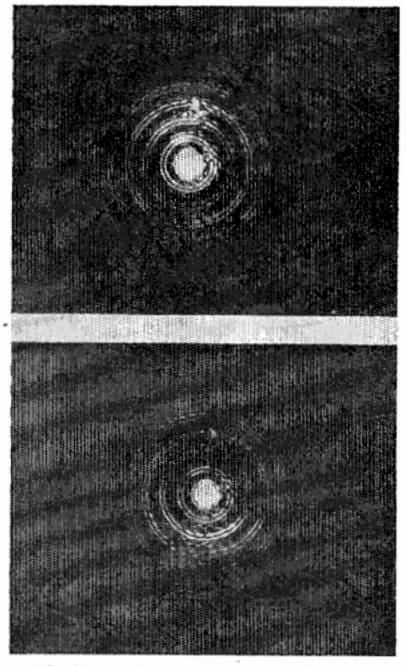

Fig. 12. Far-field diffraction pattern of the aperture of Fig. 10 showing periodic interference between the Airy patterns of the inner and outer circular apertures. The centermost region is considerably overexposed.

where δ is the average loss per bounce, assuming that all of the power is diffraction-coupled from one end of the unstable resonator. The annular output beam of the unstable resonator has a somewhat higher sidelobe level and a lower on-axis brightness than the uniformly illuminated aperture of the same outer diameter. This comparison is somewhat biased against the unstable resonator, however, since the conventional resonator is more likely to have a Guassian or other pattern which is not uniformly illuminated across the full aperture of the laser.

Discussion and Conclusion

There is obviously much more to be understood about the mode patterns and mode losses of unstable optical resonators beyond the initial results presented here. Further analytical attempts are currently in progress, particularly with the objective of developing a more detailed but still tractable analysis which will include true diffraction effects by expanding the geometrical approximation to one further order of approximation (i.e., N assumed large but not infinite). A topic of considerable practical interest on which further information is clearly needed is the possible existence of a damping or smoothing out of the repetitive periodic loss patterns versus Fresnel number seen in Figs. 7 and 8. It is hoped (and there is some tentative indication in the numerical results so far) that the *amplitude* of this ripple will decrease at larger Fresnel numbers so that the various higher-order modes will be more clearly discriminated. If this is not the case, careful selection of Fresnel number will obviously be required in any practical resonator in order to obtain maximum loss discrimination between the lowest- and higher-order transverse modes.

Another topic which has not been considered to date, but which will become important in large mode volume resonators, is the effect of spherical aberration. When the diameter of the mode is made as large as is of practical interest in, say, a ruby or CO_2 laser, the mode diameter becomes sufficiently large that the usual paraxial and parabolic approximations are no longer fully valid. What corrections this may require in the analysis are not yet known.

A third difficulty is that in large mode volume resonators of practical interest, even the basic Fresnel approximation made in deriving the integral equation in the form of (1) is no longer valid because the condition $N \ll (d/a)^2$ is not met. Because dropping this approximation considerably complicates the analysis and the presentation of results, we have concentrated to date on attempting to understand more fully the results of the analysis within the Fresnel approximation, leaving further corrections to be made at a later time.

In conclusion, the lowest- and higher-order modes in unstable optical resonators and lens waveguides can now be at least approximately understood, and the higher-order transverse modes in these systems are considerably different from the higher-order modes of more familiar stable optical systems. The phases of these waves are well described by the simple spherical wave picture, while the amplitudes are less well described by the geometrical results. It appears that such unstable optical resonators can exhibit large mode volumes and large transverse mode selection with moderate diffraction losses. Unstable resonators of this type may provide desirable resonator configurations for practical high-gain diffraction-coupled optical masers.

Acknowledgment

The authors gratefully acknowledge an illuminating conversation with Dr. J. Burch of the National Physical Laboratory, Teddington, England, during which he pointed out the eigenfunctions of (8). Contributions in the earlier stages of this project were made by J. O'Brien, and much computational assistance was given by Mrs. Cora Barry

References

[1] H. Kogelnik, "Modes in optical resonators," in *Lasers*, vol. 1, A. K. Levine, Ed. New York: Marcel Dekker, 1966, p. 295.
[2] A. E. Siegman, "Unstable optical resonators for laser applications," *Proc. IEEE*, vol. 53, pp. 277–287, March 1965.
[3] A. G. Fox and T. Li, "Resonant modes in a maser interferometer," *Bell Sys. Tech. J.*, vol. 40, pp. 453–488, March 1961.
[4] ——, "Modes in a maser interferometer with curved mirrors," in *Quantum Electronics III*, vol. 2, P. Grivet and N. Bloembergen, Eds. New York: Columbia University Press, 1964, p. 1263.
[5] A. I. Mahan, C. V. Bitterli, and S. M. Cannon, "Far-field diffraction patterns of single and multiple aperatures bounded by arcs and radii of concentric circles," *J. Opt. Soc. Am.*, vol. 54, pp. 721–732, June 1964.
[6] W. K. Kahn, "Unstable optical resonators," *Appl. Optics*, vol. 5, pp. 407–413, March 1966.
[7] S. R. Barone, "Optical resonators in the unstable region," *Appl. Optics* (submitted for publication).